An analysis of the superplastic forming of a thin circular diaphragm

Article *in* International Journal of Mechanical Sciences · May 1995

Impact Factor: 2.03 · DOI: 10.1016/0020-7403(94)00081-T

2 authors, including:

Farid Enikeev
Ufa State Petroleum Technolo…

54 PUBLICATIONS **233** CITATIONS

SEE PROFILE

Pergamon

Int. J. Mech. Sci. Vol. 37, No. 5, pp. 473–483, 1995
Elsevier Science Ltd
Printed in Great Britain
0020–7403/95 $9.50 + 0.00

0020–7403(94)00081–6

AN ANALYSIS OF THE SUPERPLASTIC FORMING OF A THIN CIRCULAR DIAPHRAGM

F. U. ENIKEEV and A. A. KRUGLOV

Institute for Metals Superplasticity Problems, R.F. Academy Sciences, Khalturina, 39, Ufa, 450001, Russian Federation

(*Received* 17 *July* 1992; *and in revised form* 4 *January* 1992)

Abstract—A new engineering model for the superplastic forming of domes has been developed. Unlike the well-known Jovane's model [1], it allows one to predict the thickness distribution of the domes. The approach involved permits the calculation of the pressure–time cycle and the thickness distribution without complicated numerical calculations. The superplastic bulge forming of domes was used as a test case. In spite of the simplicity of the model suggested, good agreement between the theoretical predictions and experimental data and results known from the literature was obtained.

NOTATION

h_p	dome height
$H = h_p/R_0$	relative dome height
$\bar{h} = h/h_p$	relative height of the dome point under consideration
R_0	die radius
R	radius of the dome
SPF	superplastic forming
s	current thickness of the dome
s_0	specimen thickness
s_b	dome thickness at the periphery
s_p	dome thickness at the apex
$s = s(\varphi, \alpha)$	thickness distribution
s_{id}	ideal thinning, corresponding to F. Jovane's model prediction [1]
$\bar{s} = s/s_{id}$	thinning factor
p	forming pressure
$\bar{p} = pR_0/\sigma_e s_0$	normalized pressure
t	time
t_f	forming time at p_f = constant

Greek letters

α	half the angle subtended by a dome surface at its center of curvature
$\dot{\varepsilon}_m, \dot{\varepsilon}_t, \dot{\varepsilon}_s$	meridian, circumferential and normal strain rate, respectively
$\dot{\varepsilon}_p$	effective strain rate at the dome apex
$\dot{\varepsilon}_0$	optimal superplastic strain rate for given material
$v = \rho_0/R_0$	numerical parameter, specified at the dome point under consideration ($0 \, v \, 1$)
ρ	distance between M′ and the symmetry axis ($t > 0$)
ρ_0	distance between M and the symmetry axis ($t = 0$)
σ_s	flow stress, corresponding to $\dot{\varepsilon}_0$
σ_p	effective stress at the dome apex
σ_m, σ_t	principal meridian and circumferential stresses, respectively
$\tau = \dot{\varepsilon}_0 t$	normalized time
φ	angle between the symmetry axis and the dome radius, drawing to the point M′ under consideration.

1. INTRODUCTION

Industrial applications of superplastic forming (SPF) require the appropriate choice of the technological parameters, which may be made on the basis of adequate theoretical techniques. The closed die set spacing, high temperatures, presence of a confining medium or vacuum restrict the applicability of all procedures for SPF process control.

Jovane [1] produced the first engineering model. It enables one to obtain the analytical expressions for the stress and strain state on the basis of membrane theory and elementary

geometrical considerations. Jovane's model does not consider the thickness non-uniformity of the dome; nevertheless, it makes possible the conclusion that the gas pressure should be varied according to a special, previously calculated program in order to maintain the deformation in an optimum superplastic range. The necessity of taking into consideration the thickness distribution and a more correct calculation of the pressure–time cycle has led to the development of various numerical analyses, including finite element methods for SPF processes [2–10]. These approaches are characterized by sufficient accuracy in the modeling; however, considerable computation time is required for their execution and, therefore, numerical methods are not always convenient in engineering practice.

In this connection it is interesting to improve Jovane's model in order to eliminate its major limitation: the neglect of thickness non-uniformity. The supposition that dome thickness is uniform is inconsistent with numerous experimental data and leads to the following contradiction at the dome periphery. Since the die does not deform during forming, the circumferential deformation along the periphery is negligible. At the same time, in accordance with the above-mentioned supposition, meridian and circumferential deformations must be equal to each other, so the latter does not vanish. That is why another assumption should be made instead of the one used by Jovane.

In the present work the following hypothesis is proposed. Every meridian passing the dome apex is assumed to be uniformly stretched at any of its point. This proposal enables one to develop a new geometrical model of the process under consideration (see Section 4). It should be mentioned that the thickness distribution [Eqn (24)] obtained on the basis of this proposal is independent of the material properties, in particular of the strain rate sensitivity m. At the same time it is well known that the deformation gradient produced during superplastic forming of domes decreases as the value of the strain rate coefficient m increases [2]. The comparison of the thickness distribution [Eqn (24)] with experimental data obtained at different strain rates results in the conclusion that the experimental values are closer to the theoretical curve, the greater the value of strain rate coefficient m. Therefore, the above-mentioned proposal seems to be valid for the optimum strain rate range only. From this follows the following limitations on the application of the new model. It seems to be applicable at high homologous temperatures ($T > 0.4\ T_{melt}$), relatively low strain rates, corresponding to the superplastic range of the material involved, and for sheet materials with isotropic fine-grained microstructures (grain size $d < 10\ \mu m$).

Besides the above-mentioned hypothesis the presented approach is based upon the following assumptions. (1) The material being bulged is isotropic and incompressible. (2) The geometry of the median plane of the formed dome is equivalent to part of a sphere at any instant of deformation. (3) At the periphery, the diaphragm is rigidly clamped, the specimen thickness being very small compared to the die radius. (4) Bending and shearing effects are neglected and membrane theory is assumed. (5) The strain rates used are relatively low so that the inertia forces can be neglected entirely; the state of stress can be determined from the equilibrium and boundary conditions.

2. EXPERIMENTAL PROCEDURE

2.1. *Installation description*

Test forming was carried out on model domes. The model dome was a hemisphere of 35 mm radius, formed from a 1 mm thick sheet VT6 (Ti–6Al–4V) titanium alloy. The SPF laboratory installation included: a heating furnace, an automatic system of gas pressure supply, a forming device and a die set.

The die set is connected to the forming device, which is schematically represented in Fig. 1. The device operation is terminated upon registration of an electric signal which arises when the forming sheet contacts an electrical indicator. The electrical indicator is placed at the center of the die cavity bottom. The die cavity is 70 mm in diameter and 35 mm in height, so the forming sheet assumes a hemispherical shape at the control time. The device includes a centering bush (7) placed at the die cavity bottom. An electrode (8) is inserted into the bush. The conical end of the electrode is directed towards the forming sheet (2), while the other end is connected to a battery (5) by means of an electrical conductor (6).

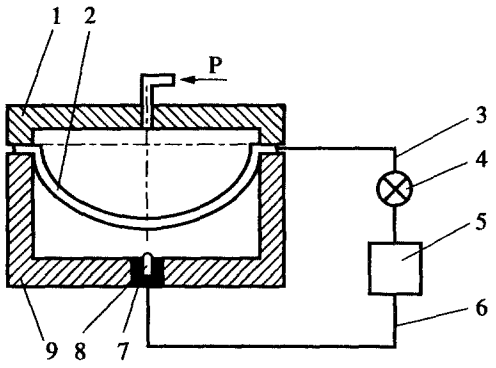

Fig. 1. Scheme of the forming estimation device.

The battery (5) is connected to the signal element (4), which in turn contacts the forming sheet (2), clamped between a female die (9) and a plate (1) through an electrical conductor (3). The centering bush is made from an insulator, while the conical rod is made from a heat-resistant alloy, in accordance with the forming temperature range. The conical end of the electrode protrudes from the working surface by 0.1–0.3 mm, which ensures the reliable registration of the contact dome apex with the die bottom.

Experimental specimens consisted of two circular sheets of 100 mm diameter packed and welded along their perimeter. One of the sheets had an adapter for the supply of forming gas. A wedge joint was used to fix the specimen flange.

The first series of experiments was performed to determine the material constants. Experiments were carried out at 900 C and constant forming pressure. The results obtained were as follows: with forming pressures of 0.5, 0.7 and 1.0 MPa the corresponding forming times turned out to be 1500, 685 and 300 sec, respectively.

The second series of experiments were to test the theoretically predicted pressure-time cycles and the thickness distribution throughout the dome profile. Specimens were formed at 900 C according to the pressure–time cycles calculated for various strain rates. The forming time was measured as the time required for the dome to touch the die cavity bottom. Experimental results are presented in Table 1. The thickness of the dome was measured along two different directions by means of a micrometer providing an accuracy of about 0.01 mm.

2.2. *Material constant determination*

Material constants for superplastic materials are usually determined using tension tests [9–11]. In practice it is rather difficult to provide identical conditions in the one-dimensional tension test conditions and the SPF process ones. Therefore, the values of material constants for sheet materials to be superplastically formed seem to be more reasonably determined on the basis of the forming test experimental data.

Let us consider free forming of a circular membrane. Initial (at $t = 0$) and current (at $t > 0$) dome profiles are shown in the Fig. 2. The current half arc length of any meridian passing through the dome apex is equal to $R\alpha$. Here, R is the dome radius, and α is half the angle subtended by the dome surface at the center of curvature. Since the initial half arc length of the meridian under consideration equals the die radius R_0, it is stretched $R\alpha/R_0 = \alpha/\sin\alpha$ times (because $R = R_0 \sin\alpha$). Proceeding from symmetry, it follows that the principal positive strains are equal to each other at the dome apex. On the other hand, any two mutually perpendicular meridians crossing at the dome apex are stretched by $\alpha/\sin\alpha$ times. Thus, proceeding from the material's incompressibility it follows that the dome thickness at the apex s_p equals

$$s_p = s_0 \cdot (\sin\alpha/\alpha)^2. \tag{1}$$

Let us now write the incompressibility condition through principle strain rates as follows:

$$\dot{\varepsilon}_m + \dot{\varepsilon}_t + \dot{\varepsilon}_s = 0, \tag{2}$$

Table 1. Experimental results

Strain rate $\dot{\varepsilon}(s^{-1})$	Flow stress σ(MPa)	Forming time (calculated) (t_1)	Forming time (measured) ($t_{1\,exp}$)	Error (%)
$2.4 \cdot 10^{-4}$	11.4	62 min 43 s	45 min 45 s	37
$4 \cdot 10^{-4}$	14.0	37 min 36 s	39 min 56 s	6
$8 \cdot 10^{-4}$	19.0	18 min 48 s	19 min 50 s	5
$1.2 \cdot 10^{-3}$	23.0	12 min 30 s	14 min 00 s	11
$4 \cdot 10^{-3}$	38.0	3 min 46 s	3 min 15 s	16

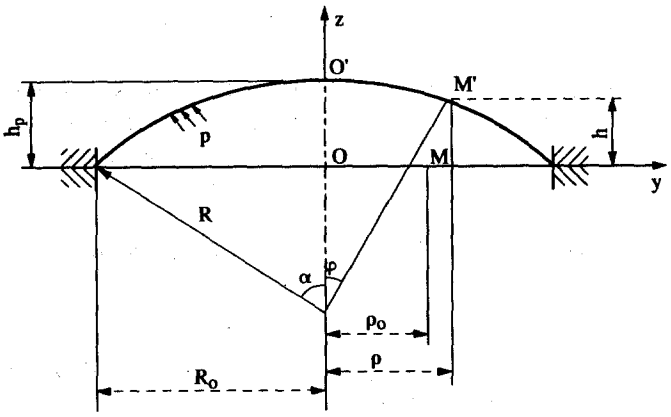

Fig. 2. Schematic for deformation modeling.

where $\dot{\varepsilon}_m$ is the meridian strain rate, $\dot{\varepsilon}_t$ is the circumferential strain rate, and $\dot{\varepsilon}_s$ is the normal strain rate.

From symmetry it follows that at the dome apex $\dot{\varepsilon}_m = \dot{\varepsilon}_t$. Thus, from Eqn (2) one may obtain $\dot{\varepsilon}_m = \dot{\varepsilon}_t = -0.5\dot{\varepsilon}_s$. The effective strain rate $\dot{\varepsilon}_p$ at the dome apex can be found as follows:

$$\dot{\varepsilon}_p = \sqrt{2\dot{\varepsilon}_{ij}\dot{\varepsilon}_{ij}/3} = |\dot{\varepsilon}_s| = -\dot{s}_p/s_p. \tag{3}$$

From Eqns (1) and (3) it follows that

$$\dot{\varepsilon}_p = -\dot{s}_p/s_p = 2\dot{\alpha}(1/\alpha - \mathrm{ctg}\alpha). \tag{4}$$

From symmetry it follows that the following relationships hold at the dome apex:

$$\sigma_p = \sigma_m = \sigma_t = pR/2s_p, \tag{5}$$

where σ_m and σ_t are the principal meridian and circumferential stresses at the dome apex, respectively, p is the value of the forming pressure, s is the current thickness of the dome, and σ_p is the effective stress at the apex.

The well-known relationship for a non-linear viscous material is assumed as follows:

$$\sigma_s = K \cdot \dot{\varepsilon}^m, \tag{6}$$

where K and m are the material constants of the alloy involved for the given temperature. It should be noted that Eqn (6) assumed in the present work means that, in logarithmic coordinates, the $\ln(\sigma_s)$ versus $\ln(\dot{\varepsilon})$ dependence is represented by a straight line. At the same time it is well known [9–11] that in reality a sigmoidal variation of the flow stress with strain rate takes place. Thus, Eqn (6) may be applied only as the local approximation describing the sigmoidal curve within a rather narrow range of the strain rates. From this it follows that, in order to determine the concrete values of material constants K and m, the

test forming should be carried out with such values of forming pressure that the strain rate range corresponds to the given one.

Substituting Eqns (1) and (6) into Eqn (5) and taking into consideration that $R = R_0/\sin\alpha$, one can obtain that

$$p = (2s_0/R_0)\cdot K\cdot(\sin^3\alpha/\alpha^2)\cdot[2\dot{\alpha}(1/\alpha - \operatorname{ctg}\alpha)]^m = p_0 = \text{const.} \tag{7}$$

It is easily seen that Eqn (7) is an ordinary differential equation of the first order for the unknown function $\alpha(t)$. Integrating Eqn (7) one can obtain

$$(p_0R_0/2s_0K)^{1/m}t = 2I_m(\alpha), \tag{8}$$

where

$$I_m(\alpha) = \int_0^{\alpha}[(\sin^3 x/x^2)]^{1/m}\cdot(1/x - \operatorname{ctg} x)\mathrm{d}x. \tag{9}$$

Unfortunately, the integral on the right side of Eqn (9) is not expressed through elementary functions; however, it can be easily calculated numerically. Thus, the α versus time dependence can be obtained. On the basis of known dependence $\alpha(t)$ it is easy to obtain the time dependencies of the relative dome height $H = \operatorname{tg}(\alpha/2)$, dome radius $R = R_0/\sin\alpha$ and the dome thickness at the apex s_p from Eqn (1).

From Eqn (8) it follows that material strain rate sensitivity m may be defined from the following expression:

$$m = \ln(p_1/p_2)/\ln(t_2/t_1), \tag{10}$$

where t_1 and t_2 are forming times at constant pressures p_1 and p_2, respectively. The parameter K may be calculated from the expression:

$$K = (p_fR_0/2s_0)\cdot[t_f/2I_m(\pi/2)]^m, \tag{11}$$

where t_f is the forming time at constant pressure $p_f = \text{const.}$; $I_m(\pi/2)$ should be calculated numerically from Eqn (9) with a value of m, determined according to Eqn (10). In Fig. 3, $I_m(\pi/2)$ values calculated in accordance with Eqn (9) are plotted versus m. Calculations according to Eqn (10) for any two experimental pairs of pressure, p_f, and forming time, t_f, values give $m = 0.43$. With $m = 0.43$ and $\alpha = \pi/2$ from Eqn (9) it follows that $I_m(\pi/2) \cong 0.0983$. Then, from Eqn (11) one can obtain $K \cong 410\ \text{MPa}\cdot\text{c}^{-m}$.

In Fig. 4 the time dependence of the relative dome height H is presented. The values of $H = \operatorname{tg}(\alpha/2)$ were calculated according to Eqn (8) with K, m determined from the experiments. The behavior of the $H(t)$ curves is similar to that of the experimental ones [5, 8], while the calculated forming time practically coincides with that measured experimentally.

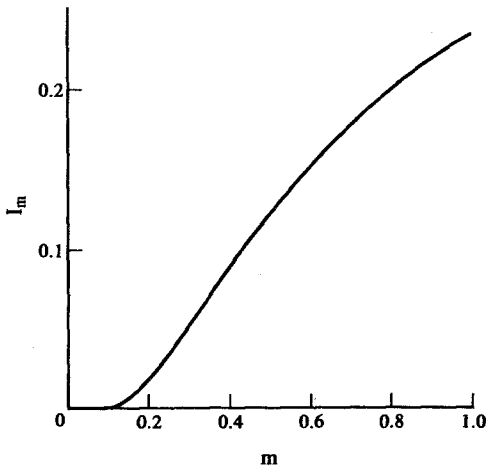

Fig. 3. Calculated values of $I_m(\pi/2)$ vs material strain rate sensitivity m.

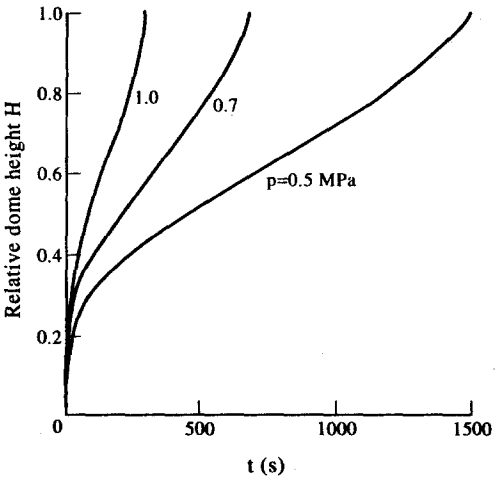

Fig. 4. Time dependencies of the relative dome height for testing forming with constant pressure p (the numbers near curves mean the values of gas pressure in MPa).

3. PRESSURE–TIME CYCLE CALCULATION

It is known [9–11] that superplastic deformation is realized only in a narrow strain rate range. In order to provide the superplastic regime of forming we assume that the effective strain rate at the dome apex $\dot{\varepsilon}_p$ is constant and is equal to some given value $\dot{\varepsilon}_0$, corresponding to the superplastic range of the material involved:

$$\dot{\varepsilon}_p = \dot{\varepsilon}_0 = \text{const.} \tag{12}$$

To satisfy condition (12) the forming pressure should be strictly related to time. From Eqn (5) it follows that

$$p = (2s_p/R)\,\sigma_p. \tag{13}$$

To obtain a concrete form for the function $p(t)$, let us find the time dependencies of all variables on the right side of Eqn (13) from the condition (12):

Substituting Eqn (6) into Eqn (12) one finds that $\sigma_p = \sigma_s = \text{const.}$, where σ_s is flow stress corresponding to the given strain rate $\dot{\varepsilon}_0$. In order to find the time dependence of the dome thickness at apex s_p let us substitute Eqn (3) into Eqn (12). After integrating one can obtain;

$$s_p(t) = s_0 \exp(-\dot{\varepsilon}_0 t). \tag{14}$$

It should be noted that Eqn (14) is valid not only for free forming, but for deformation as well. For the sake of simplicity we shall further consider a cylindrical die.

The time dependence of the dome radius during deforming into a die is obvious: $R(t) = R_0$. In order to obtain $R(t)$ for free forming one can take into consideration, that, in accordance with Eqns (2), (3) and (12), the meridian strain rate $\dot{\varepsilon}_m$ is equal to

$$\dot{\varepsilon}_m = (1/R\alpha)\mathrm{d}(R\alpha)/\mathrm{d}t = -0.5\dot{\varepsilon}_s = 0.5\dot{\varepsilon}_0. \tag{15}$$

It should be noted that, at the initial moment of time $t = 0$, $R = \infty$, $\alpha = 0$, but $R\alpha = R_0$. Integrating Eqn (15) and taking in mind that $R = R_0/\sin\alpha$, one may obtain the following transcendental equation for the unknown function $\alpha = \alpha(t)$:

$$\alpha/\sin\alpha = \exp(\dot{\varepsilon}_0 t/2). \tag{16}$$

The following approximate solution of Eqn (16) may be recommended for practical use:

$$\alpha(t) \cong \sqrt{3\dot{\varepsilon}_0 t}. \tag{16'}$$

Its inaccuracy does not exceed 6% (when $0 \leqslant \alpha \leqslant \pi/2$).

At some moment of time $t = t_1$, defined from the condition $\alpha(t_1) = \pi/2$, the dome shape becomes hemispherical and further deformation will be developed without the shape changing and a cylindrical contact zone will be developed. Substituting the condition $\alpha(t_1) = \pi/2$ into Eqn (16) one may deduce that the forming time equals:

$$t_1 = (2/\dot{\varepsilon}_0) \cdot \ln(\pi/2) \cong 0.9/\dot{\varepsilon}_0. \tag{17}$$

Thus, time dependence of the forming pressure has the form of Eqn (13), where $s_p(t)$ comes from Eqn (14), $R(t) = R_0/\sin\alpha$ when $0 \leqslant t \leqslant t_1$ and $R(t) = R_0$ when $t > t_1$. From Eqns (13), (14) and (16) it follows that the pressure–time cycle may be calculated in accordance with the following analytical expression:

$$p(t) = \begin{cases} (2s_0/R_0) \cdot \sigma_s \cdot \sin\alpha \cdot \exp(-\dot{\varepsilon}_0 t) & \text{when } 0 \leqslant t \leqslant t_1 \\ (2s_0/R_0) \cdot \sigma_s \cdot \exp(-\dot{\varepsilon}_0 t) & \text{when } t > t_1 \end{cases} \tag{18}$$

where t_1 is from Eqn (17), σ_s is the flow stress corresponding to the given strain rates $\dot{\varepsilon}_0$, $\alpha(t)$ is from Eqn (16) or (16′). In Fig. 5 the dependence $p(t)$ from (19) is represented in non-dimensional coordinates $\bar{p} - \tau$, where $\bar{p} = pR_0/\sigma_e s_0$ and $\tau = \dot{\varepsilon}_0 t$. A dashed line is plotted on the basis of the approximate solution (16′). From Fig. 5 it follows that approximation (16′) is suitable for practical use.

In order to compare the results obtained with those of Jovane's model, let us write Eqn (18) in pressure p–relative dome height $H = \mathrm{tg}(\alpha/2)$ coordinates:

$$p = (4s_0\sigma_e/R_0) \cdot \{H^3/[(1 + H^2)^3 \cdot (\mathrm{arctg}H)^2]\} \quad \text{when } 0 \leqslant H \leqslant 1. \tag{19}$$

In Fig. 6(a) the dependence $p(H)$ from Eqn (19) is compared with an analogous Jovane model curve. It is seen that the presented pressure–time cycle differs considerably from the Jovane one. Guo and Ridley [5] have obtained $p(t)$ and $H(t)$ dependencies similar to those shown in Figs 5 and 6(b), respectively. The assumptions made by Guo and Ridley coincide with those adopted in the present work; however, their approach is more complicated and their calculations are much longer.

In Table 1, theoretical predictions [calculated according to Eqn (17)] and experimentally measured forming times are presented. The values of the flow stress σ_s and relative error (%) are presented as well. It is seen that the largest disagreements are obtained at the boundaries of the strain rate interval under study, which confirms the above note as to the limitation on the interval of applicability of the constitutive equation of the form of Eqn (6) (see end of Section 2).

On the other hand, if one had a reliable stress–strain rate curve $\sigma(\dot{\varepsilon})$ at one's disposal, the necessity of carrying out the test forming would disappear. In this case the value of σ_s which

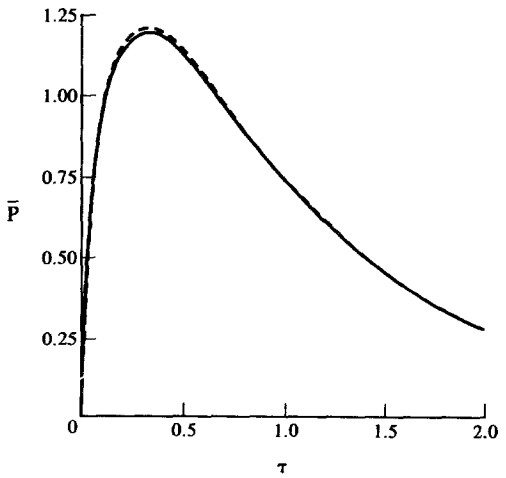

Fig. 5. Calculated pressure–time cycle (normalized values $\bar{p} = pR_0/\sigma_s s_0$ and $\tau = \dot{\varepsilon}_0 t$). Solid line corresponds to the strict solution; dashed line to the approximate solution.

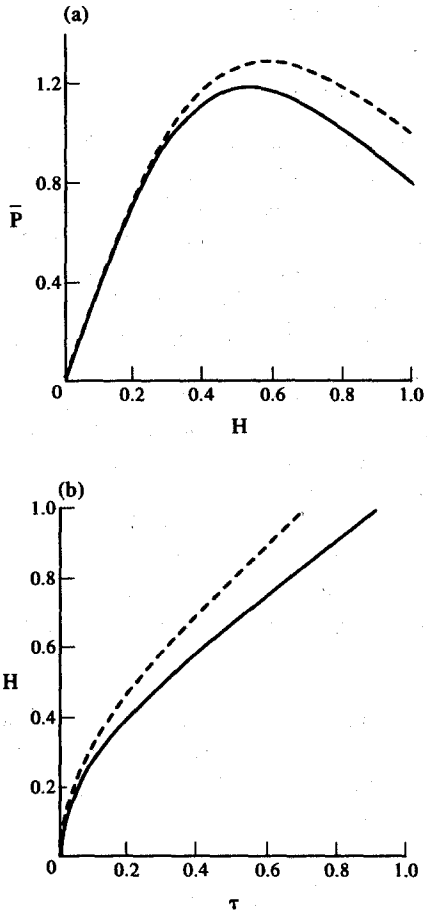

Fig. 6. Dependence of normalized pressure $\bar{p} = pR_0/\sigma_s s_0$ on the relative dome height H (a) and dependence of relative dome height H on normalized time $\tau = \dot{\varepsilon}_0 t$ (*b*). Solid line corresponds to the solution suggested; dashed line corresponds to that of Jovane [1].

is to be substituted into Eqn (18) would be found immediately from the experimental stress–strain rate curve $\sigma(\dot{\varepsilon})$ for the given strain rate $\dot{\varepsilon}_0$. It should be emphasized that in this case the optimal superplastic strain rate $\dot{\varepsilon}_0$ and corresponding effective stress σ_s would be considered as the material's constants in calculating the pressure–time cycle.

If one wished to take into consideration the influence of grain growth on the pressure–time cycle this could be done by means of introducing a time-dependent σ_s into Eqn (18).

4. THICKNESS DISTRIBUTION

As obtained above (see Section 2.2) the dome thickness at the apex s_p may be appreciated from Eqn (1). Let us now consider the principles of thinning along the periphery of the dome. Since the clamp does not deform during forming, the circumferential deformation along the periphery is negligible. On the other hand, any meridian approaching the periphery is stretched by $\alpha/\sin\alpha$ times. From this it follows that dome thickness at the periphery s_b is equal to

$$s_b = s_0 \cdot \sin\alpha/\alpha. \tag{20}$$

It should be noted that the Jovane model contains the following contradiction: circumferential deformation along the periphery has to vanish while in accordance with Jovane's assumptions meridian and circumferential deformations must be equal to each other, so the latter does not vanish.

If thinning were uniform along the dome profile (as for the Jovane model) the dome thickness s_{id} would be equal to

$$s_{id} = s_0/(1 + H^2) = s_0 \cos^2(\alpha/2). \tag{21}$$

It is easy to see that $s_b \geqslant s_{id} \geqslant s_p$ when $0 \leqslant \alpha \leqslant \pi/2$. From this it follows that there is such a thickness distribution $s = s(\varphi, \alpha)$ that the dome volume equals the initial volume of the diaphragm and $s(0, \alpha) = s_p$, $s(\alpha, \alpha) = s_b$. In order to obtain the thickness distribution $s = s(\varphi, \alpha)$ let us consider a new geometrical model of the process under consideration. The basic assumption of this model is that each meridian at any of its points is stretched by $R\alpha/R_0 = \alpha/\sin\alpha$ times. This assumption was already used in Section 2.1 in obtaining Eqn (1). This assumption seems to be valid for the optimum superplastic strain rate range (see the discussion below of Fig. 8).

Let us choose a certain point M of the initial diaphragm which at $t = 0$ is at distance $\rho_0 = vR_0$ from the point 0 (Fig. 2). Here, v is the number characterizing the initial position of the dome point under consideration, $0 \leqslant v \leqslant 1$. At some moment of time $t > 0$ the point M transfers to point M′, and point 0 to 0′. Let φ be the angle between the symmetry axis and the dome radius drawn to the point M′ under consideration. The value of φ determines the position of the dome point under consideration; in particular, $\varphi = 0$ corresponds to the dome apex, while $\varphi = \alpha$ corresponds to the periphery. Since M and M′ correspond to the same material point, the following relationship between parameters φ and v holds:

$$\varphi = v\alpha. \tag{22}$$

The meridian passing the point M′ is stretched by $\alpha/\sin\alpha$ times. The latitude passing the point M′ is stretched by ρ/ρ_0 times, where ρ is the distance between M′ and the symmetry axis ($t > 0$) and ρ_0 is the distance between M and the symmetry axis ($t = 0$). From this it follows that the dome thickness at the point M′ may be found as follows (incompressibility condition is assumed):

$$s/s_0 = (\rho_0/\rho) \cdot (\sin\alpha/\alpha). \tag{23}$$

Taking into account that $\rho = R\sin\varphi$, $\rho_0 = vR_0$ from Eqns (22) and (23) one can obtain

$$s(\varphi, \alpha) = s_0[\sin(\alpha)/\alpha]^2 \varphi/\sin\varphi. \tag{24}$$

Equation (24) gives the dome thickness at the point determined by the value of φ for the configuration determined by a value of α. It is easy to see that Eqn (24) satisfies the following boundary conditions: $s(0, \alpha) = s_p$, $s(\alpha, \alpha) = s_b$, where s_p and s_b are the dome thicknesses at the apex and at the periphery, respectively.

In order to analyze the result obtained, let us introduce a relative dome thickness (or the so-called "thinning factor" [2, 3, 8]) $\bar{s}(\varphi, \alpha) = s(\varphi, \alpha)/s_{id}$, where $s_{id} = s_0\cos^2(\alpha/2)$ corresponds to the ideal thinning of Jovane [Eqn (21)]. The thinning, determined by Eqn (24) may be called a geometrical one. The angular position φ^* of the dome point where the geometrical thinning is equal to the ideal one may be determined from the condition $\bar{s}(\varphi, \alpha) = 1$. From Eqn (24) it follows that $\varphi^* = \varphi^*(\alpha)$. In particular, for a hemisphere $\alpha = \pi/2$, $\varphi^* = 63°$, $\cos\varphi^* = 0.454$, $v^* = 0.7$. Cornfield and Johnson [2] have experimentally and numerically obtained the dependence $\bar{s}(\varphi, \pi/2)$ at coordinates $\bar{s}$ and $\cos\varphi$ and found that $\bar{s} = 1$ when $\cos\varphi = 0.45$. Smirnov [9] has found that $\bar{s} = 1$ when $v = 0.7$. Thus, the present model rightly predicts the location of the dome point in which the geometrical thinning is equal to the ideal one.

In order to draw the dependence of the relative dome thickness (thinning factor) $\bar{s}$ versus relative height of the dome point under consideration at various values of dome height h_p, we write:

$$\frac{h}{h_p} = \frac{\cos\varphi - \cos\alpha}{1 - \cos\alpha}$$
$$\bar{s}(\varphi, \alpha) = \left(\frac{\sin(\alpha/2)}{\alpha/2}\right)^2 \frac{\varphi}{\sin\varphi} \tag{25}$$

In Fig. 7, $\bar{s}(\bar{h})$, calculated in accordance with Eqn (25) for various values of the relative dome height $H = h_p/R_0 = \mathrm{tg}(\alpha/2)$, are represented. The curves obtained are similar to those reported by other investigators [2, 3].

In Fig. 8 the theoretical thickness distribution calculated for a model dome ($R_0 = 35$ mm, $s_0 = 1$ mm, $H = 1$, $\alpha = \pi/2$) is shown. For the sake of comparison, experimental values of the hemisphere's thickness formed at 900 C from the titanium alloy VT6 at different strain rates are represented as well. From Fig. 8 it follows that the experimental values of the hemisphere's thickness deformed at $\dot{\varepsilon} = 4{\cdot}10^{-4}\ \mathrm{s}^{-1}$, which corresponds to the optimal strain rate range, are closer to the theoretical curve. Thus, the supposition that each meridian at any of its points is stretched by $R\alpha/R_0 = \alpha/\sin\alpha$ times seems to be valid for the optimum strain rate range only. On the other hand, this supposition means that the localization of deformation does not arise, which agrees with the well-known fact that superplastic deformation is characterized by the material's ability to lengthen abnormally without necking only in the optimum strain rate range [9–11]. At the same time it is known that as the value of strain rate sensitivity decreases the localization of deformation becomes more prevalent.

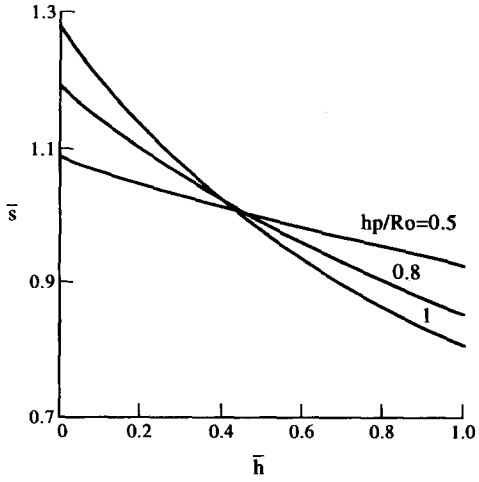

Fig. 7. Thinning factor $\bar{s}$ vs relative height of the dome point under consideration $\bar{h} = h/h_p$ for different relative dome height h_p/R_0 (the numbers near curves).

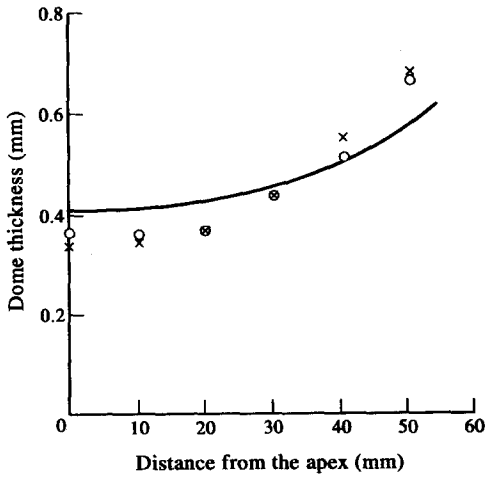

Fig. 8. Theoretical dependence of the dome thickness on the distance from the dome apex (along the meridian) — solid line. Experimental points—the thickness of the domes, obtained in forming with constant strain rate: xxx — $\dot{\varepsilon} = 1.2{\cdot}10^{-3}\ \mathrm{s}^{-1}$; ○○○ — $\dot{\varepsilon} = 4{\cdot}10^{-4}\ \mathrm{s}^{-1}$.

It should be noted that, on the basis of the model presented, the deformation of a circular diaphragm into a cylindrical or conical die may be considered. In spite of some bulkiness in the intermediate calculations, the results represent simple analytical expressions, which may be applied to predict the thickness distribution of the axisymmetric products, as well as for calculations of the initial specimen profile. The latter is necessary for obtaining the desirable thickness distribution of the products.

5. CONCLUSIONS

The free bulging of a sheet, which is clamped along around its periphery, into a female cylindrical mold has been considered. A new engineering model of SPF of a circular diaphragm has been developed. Retaining the simplicity of Jovane's model the suggested one is based upon another geometrical model of the process under consideration. It allows one to evaluate the thickness distribution and calculate a pressure–time cycle, taking this factor into consideration.

The main proposal of the model suggested is that every meridian passing through the dome apex is uniformly stretched at any moment of time. The comparison between the theoretical thickness distribution [Eqn (24)] and the experimental data, which was obtained at different strain rates, leads to the conclusion that this proposal seems to be valid for the optimum strain rate range only. It should be emphasized that the thickness distribution [Eqn (24)] does not depend on the material properties and seems to be valid for superplastic materials with relatively high strain rate sensitivity m, for example, for fine-grained titanium alloys.

The optimal superplastic strain rate $\dot{\varepsilon}_0$ and corresponding effective stress σ_s may be considered as the material constants in calculating the pressure–time cycle in accordance with Eqn (19). If the values of $\dot{\varepsilon}_0$ and σ_s are not known in advance, they may be found on the basis of test formings as described in Section 2.2. The technique developed in this section, enables one to determine the material constants K and m, for the well-known relationship for a non-linear viscous fluid $\sigma = K \cdot \dot{\varepsilon}^m$ on the basis of the results of constant pressure test forming. The main advantage of this technique is to identify the testing conditions for the SPF process. It should be emphasized that the approximation of stress–strain rate dependence in the form $\sigma = K \cdot \dot{\varepsilon}^m$ is valid only within a narrow strain rate interval, because in reality a sigmoidal variation of the flow stress with strain rate takes place. Table 1 is a good illustration of the narrowness of the relationship $\sigma = K \cdot \dot{\varepsilon}^m$.

REFERENCES

1. F. Jovane, An approximate analysis of the superplastic forming of a thin circular diaphragm: theory and experiments. *Int. J. Mech. Sci.* **10**, 403 (1968).
2. G. G. Cornfield and R. H. Johnson, The forming of superplastic sheet materials. *Int. J. Mech. Sci.* **12**, 479 (1970).
3. H. S. Yang, H. K. Ahmed and W. T. Roberts, Process control of superplastic forming under superimposed hydrostatic pressure. *Mater. Sci. Engng* **A122**, 193 (1989).
4. D. Y. Yang and T. S. Noh, An analysis of hydroforming of longitudinally curved boxes with regular polygonal cross-section. *Int. J. Mech. Sci.* **32**, 877 (1990).
5. Z. X. Guo and N. Ridley, Modeling of superplastic bulge forming of domes. *Mater. Sci. Engng* **A114**, 97 (1989).
6. Y. J. Kim and D. Y. Yang, A. rigid–plastic finite element formulation considering the effect of geometric change and its application to hydrostatic bulging. *Int. J. Mech. Sci.* **27**, 453 (1985).
7. M. Bellet and J. L. Chenot, Numerical modeling of thin sheet superplastic forming. *Proc. 3rd Int. Conf.*, Fort Collins, CO, p. 401 (1989).
8. H. S. Yang and A. K. Mukherjee, An analysis of the superplastic forming of a circular sheet diaphragm. *Int. J. Mech. Sci.* **34**(4), 283 (1992).
9. O. M. Smirnov, *Pressure Metals Treatment in Superplastic State*, Mashinostroyenie, Moscow (1979) (in Russian).
10. *Superplastic Forming of Structural Alloys* (edited by N. E. Paton and C. H. Hamilton) TMS, Warrendale, PA (1982).
11. O. A. Kaibyshev, *Structural Alloys Superplasticity*, M.: Metallurgiya (1984) (in Russian).